

1 **Long-term trends in the distribution of ocean**
2 **chlorophyll**

3 **Dongran Zhai ¹, Claudie Beaulieu ¹, Raphael M. Kudela ¹**

4 ¹University of California, Santa Cruz, 1156 High St, Santa Cruz, CA 95064

5 **Key Points:**

- 6 • Long-term changes are detected in different aspects of the distribution of chlorophyll-
7 a (not just the mean state).
8 • Oceanic chlorophyll-a high extremes are changing faster than chlorophyll-a mean
9 globally during 1997-2022.
10 • On a regional scale, chlorophyll-a extremes trends are predominant at high lat-
11 itude (+), equatorial (-), and oligotrophic regions (-).

Corresponding author: Dongran Zhai, dzhai@ucsc.edu

Abstract

The concentration of chlorophyll-a (CHL) is an important proxy for autotrophic biomass and primary production in the ocean. Quantifying trends and variability in CHL are essential to understanding how marine ecosystems are affected by climate change. Previous analyses have focused on assessing trends in CHL mean, but little is known about observed changes in CHL extremes and variance. Here we apply a quantile regression model to detect trends in CHL distribution over the period of 1997-2022 for several quantiles. We find that the magnitude of trends in upper quantiles of global CHL (>90th) are larger than those in lower quantiles (≤ 50 th) and in the mean, suggesting a growing asymmetry in CHL distribution. On a regional scale, trends in different quantiles are statistically significant at high latitude, equatorial, and oligotrophic regions. Assessing changes in CHL distribution has potential to yield a more comprehensive understanding of climate change impacts on CHL.

Plain Language Summary

The marine environment is essential to nature and society, as it provides food and other important services such as Earth's climate regulation and habitat for species. Marine primary productivity is increasingly stressed due to global climate change. Detecting the impact of climate change on primary producers should be a priority given their critical role in the climate system. Most studies focus on the impact of climate change by evaluating the mean state of primary productivity, but little is known about whether and how climate change is impacting variance and extremes. Here we assess changes in chlorophyll-a (CHL), which is an important proxy for primary production of marine ecosystems. We quantify long-term changes in different aspects of the CHL distribution (mean, variance, and extremes) using a quantile regression model. We find that CHL high extremes and variability are slightly intensified globally during the 26 years of observational record. Trends in regional scales, especially in high-latitude and North Atlantic Subtropical Gyre, show that CHL high extremes have been increasing since 1997. Our results suggest that more emphasis should be put into understanding the impact of climate change on the variance and extremes of primary productivity for climate change adaptation and mitigation.

1 Introduction

Global climate change is increasingly affecting marine ecosystems, altering the ocean's biological primary productivity. Based on coupled model projections, a global decline in primary productivity is expected due to changes in temperature, light, nutrients, and grazing (Bopp et al., 2013; Kwiatkowski et al., 2020), with potential repercussions on marine ecosystems (Laufkötter et al., 2015), fisheries (Free et al., 2019), and the global carbon cycle (Sarmiento et al., 2004). Marine phytoplankton contribute nearly half of the global primary productivity (Field et al., 1998). Consequently, detecting the impact of climate change on marine phytoplankton should be a priority given the critical role that primary productivity play in physical and biogeochemical interactions in the ocean.

Chlorophyll-a (CHL) is an essential climate variable and an important proxy for marine primary productivity (Bojinski et al., 2014; Hollmann et al., 2013). Satellite CHL offers high temporal and spatial resolution to support global and regional assessments of long-term changes in CHL (McClain, 2009; Blondeau-Patissier et al., 2014; Bindoff et al., 2022). To date, studies of long-term trends in CHL have focused on changes in the mean state (Gregg et al., 2005; Boyce et al., 2010; Henson et al., 2010; Boyce et al., 2010; Saulquin et al., 2013; Mélin, 2016; Henson et al., 2016; Hammond et al., 2020). Although assessing long-term trends in the mean is important for understanding how CHL is changing, this does not depict a complete portrait of changes. Assessing changes in

61 variability and extremes may yield a more complete understanding of climate change im-
62 pacts on CHL.

63 Ocean extremes and their impact on marine ecosystems have sparked a lot of at-
64 tention and concern recently (Gruber et al., 2021). Marine heatwaves, low oxygen con-
65 centrations, and high acidity events are expected to intensify and occur more often, with
66 impacts on organisms and ecosystems, further affecting ecosystem services and human
67 welfare (Gruber et al., 2021). Compound extreme events, where two or more ocean ex-
68 tremes are happening synergistically (e.g., low oxygen and high temperature) are of par-
69 ticular concern as they can contribute to biological and ecological impacts in different
70 ways (Gruber et al., 2021; Le Grix et al., 2021; Burger et al., 2022). Several studies have
71 considered how the ocean’s variance may be responding to climate change, including sea
72 surface temperatures (Alexander et al., 2018), marine carbon dioxide (Landschützer et
73 al., 2018), sea ice (Tareghian & Rasmussen, 2013), sea level (Barbosa, 2008), and phy-
74 toplankton biomass (Elsworth et al., 2022). A recent study showed that changes in vari-
75 ance are omnipresent in different aspects of Earth’s climate and span physical and ecosys-
76 tem variables, and tend to be more predominant in variables that are typically not nor-
77 mally distributed such as primary production (Rodgers et al., 2021). To our knowledge,
78 there is no prior assessment of change in global CHL distribution over the observational
79 period.

80 In this study, we provide a first assessment of changes in the whole CHL distribu-
81 tion, since other aspects of the CHL distribution (e.g., extremes) may be equally or even
82 more important than the mean CHL. Our objective is to assess observed long-term trends
83 in CHL distribution globally and regionally. Two multi-mission satellite products are uti-
84 lized to expand the variety of results on global and regional scales and reduce the effect
85 of the sensitivity of datasets. The impact of seasonality is also taken into account. We
86 estimate long-term trends in multiple quantiles of a time series using quantile regression
87 (QR), which together represent spatial and temporal changes in the distribution, includ-
88 ing the tails representing extreme events (Cai & Reeve, 2013).

89 2 Data and Methodology

90 2.1 Data

91 We use two chlorophyll-a (mg/m^3) data products spanning 1997 to 2022. The first
92 one is derived from the ESA’s Ocean Color Climate Change Initiative (OC-CCI) project
93 version 6.0 (Sathyendranath et al., 2019). This is a satellite multi-mission data product
94 computed from merging the remote-sensing reflectance of a set of sensors, including Sea-
95 viewing Wide Field-of-view Sensor (SeaWiFS), Moderate Resolution Imaging Spectro-
96 radiometer onboard the Aqua (MODIS-A), Medium Resolution Imaging Spectrometer
97 (MERIS), Visible Infrared Imaging Radiometer Suite (VIIRS), and Ocean and Land Colour
98 Instrument (OLCI). The OC-CCI product is continuously corrected for biases (Mélin et
99 al., 2017). Additional analyses using the OC-CCI data product are included in the sup-
100 porting information (Text S1).

101 The second dataset is derived from the GlobColour Project of the Copernicus Ma-
102 rine Environment Monitoring Service (CMEMS). This merged chlorophyll-a product is
103 constructed by a combination of chlorophyll-a products directly computed for each sen-
104 sor (SeaWiFS, MODIS-A, MERIS, VIIRS, and OLCI) (Garnesson et al., 2019), which
105 provides a “cloud-free” product by space-time interpolation. While the focus of our anal-
106 ysis is on the OC-CCI dataset, we include additional analyses of GlobColour in the sup-
107 porting information (Text S2) as a measure of sensitivity.

108 Both datasets cover from September 1997 to December 2022 and are gridded at 4
109 km spatial resolution and monthly temporal resolutions. They have been regridded from
110 a $1/24^\circ$ grid to a 1° grid by averaging within 1 degree boxes. Before fitting the QR model,

111 the monthly data is deseasonalized in both datasets assuming a constant seasonal cycle.
112

113 2.2 Quantile Regression Model

114 To quantify changes in CHL distribution, we estimate trends in different distribution
115 quantiles via QR (Koenker & Bassett Jr, 1978). While assessing change in the mean
116 of climate variables using ordinary least squares (OLS) provides extremely valuable in-
117 formation, it does not provide insight into changing extremes and how overall variabil-
118 ity is related to time-varying events (Abbas et al., 2019). The main difference with OLS
119 is that QR substitutes the conditional mean function in OLS for a conditional quantile
120 function (Koenker & Bassett Jr, 1978; Koenker & D'Orey, 1987). As such, instead of mod-
121 eling the mean response in the regression model, QR models the response at a given quan-
122 tile level. The QR model makes no assumptions about the distribution of the target vari-
123 able and the residuals. Specifically, QR can identify opposite trends in statistical extremes
124 (upper and lower) that would remain hidden if focusing on means (Sankarasubramanian
125 & Lall, 2003). We use a QR model to assess trends of CHL in various quantile levels.
126 The model is given by:

$$y_t = \alpha_\tau + \beta_\tau t + \epsilon_{t\tau}, \quad (1)$$

127 where y_t is the response variable (i.e., CHL) at time t (in months) for the condi-
128 tional quantile τ , α_τ and β_τ denote the intercept and slope for quantile level τ , respec-
129 tively. Residuals are represented by ϵ_τ . The quantile regression model can be expressed
130 as $y = f'(\alpha_\tau, \beta_\tau, t)$. For given parameters α_τ and β_τ , they are estimated by minimiz-
131 ing the sum of asymmetrically weighted absolute residuals

$$\sum_{t=1}^n \rho_\tau(y_t - f'(\alpha_\tau, \beta_\tau, t)), \quad (2)$$

132 where n is the data length and ρ_τ represents the tiled absolute value function, which
133 gives different weights to positive and negative residuals (Koenker & Hallock, 2001). The
134 tiled absolute value function can be expressed as:

$$\rho_\tau = \begin{cases} \tau, & y_t \geq (\alpha_\tau + \beta_\tau t) \\ 1 - \tau, & y_t < (\alpha_\tau + \beta_\tau t) \end{cases} \quad (3)$$

135 We fit QR models at several quantile levels (5%, 10%, 50%, 90%, and 95% levels).
136 As a comparison, OLS is also used here to fit trends in the mean CHL. The quantile re-
137 gression model is implemented using the R package `quantreg` (Koenker et al., 2018).

138 2.3 Serially Correlated Residuals

139 Monthly chlorophyll-a concentration may exhibit serial autocorrelation in time series,
140 which may bias trend detection (Beaulieu et al., 2013). Here we assume that resid-
141 uals in CHL may follow a first-order autocorrelation (AR1) model. The quantile regres-
142 sion residuals at level τ , $\epsilon_{\tau t}$, are given by:

$$\epsilon_{\tau t} = \phi_\tau \epsilon_{\tau t-1} + \hat{\nu}_{\tau t}, \quad (4)$$

143 where ϕ is the first-order autocorrelation coefficient and $\hat{\nu}_\tau$ denotes white noise er-
144 rors.

145 QR estimates may be biased in the presence of correlated errors (Koenker et al.,
 146 2017). To verify the presence of autocorrelation in the residuals of the QR, we use a residual-
 147 based autocorrelation test, named the QF test (Huo et al., 2017). The test statistic is
 148 given by:

$$QF_T = \frac{\sum_{t=1}^T \tilde{\nu}_{\tau t}^2 - \sum_{t=1}^T \hat{\nu}_{\tau t}^2}{\sum_{t=1}^T \hat{\nu}_{\tau t}^2 / (T - p - k)}, \quad (5)$$

149 where $\hat{\nu}_{\tau t}^2$ denotes the residuals from the AR1 model fitted on the quantile resid-
 150 uals in Equation 4, implying the model under the alternative hypothesis ($H_1 : \phi \neq 0$),
 151 $\tilde{\nu}_{\tau t}^2$ denotes the residuals under the null hypothesis ($H_0 : \phi = 0$) in which all paramet-
 152 ers for lagged residuals are joint to zero under the null hypothesis, T is the length of
 153 time series, p is the autocorrelation order, and k is the number of explanatory variables.
 154 The asymptotical distribution of the QF statistic is a chi-squared distribution with p de-
 155 grees of freedom. More detailed information is presented in Huo et al. (2017).

156 If serial correlation is detected in the residuals from the QF test, we transform the
 157 time series by modifying the response variable (Cochrane & Orcutt, 1949):

$$y_t - \phi_{\tau} y_{t-1} = \alpha_{\tau} (1 - \phi_{\tau}) + \beta_{\tau} (t - \phi_{\tau} (t - 1)) + \nu_{\tau t}, \quad (6)$$

158 Where α_{τ} and β_{τ} are estimated from Equation 1. The autoregressive parameter
 159 ϕ_{τ} is estimated by first regressing the untransformed QR model and obtaining the resid-
 160 uals $\hat{\epsilon}_t$, then regressing $\hat{\epsilon}_t$ on $\hat{\epsilon}_{t-1}$. Note that the first data point is lost in this process,
 161 and there are $n-1$ residual terms $\nu_{\tau t}$ after transformation. If the transformation was suc-
 162 cessful, the $\nu_{\tau t}$ should be white noise. To account for potential sensitivity to the choice
 163 of transformation method, We also use the Hildreth-Lu procedure (Hildreth & Lu, 1960).
 164 This procedure is also a transformation based on differencing, but the Hildreth-Lu pro-
 165 cedure offers a simultaneous estimation of the autocorrelation of the disturbances and
 166 the coefficients (Dufour et al., 1980). Results using Hildreth-Lu are included in the sup-
 167 porting information (Text S1; Figure S1).

168 3 Results

169 3.1 Global Trends and Variability

170 On a global scale, trend estimates vary according to quantile levels (Figure 1). The
 171 magnitude of trend in the upper quantile of global CHL (95th) is larger than those in
 172 the middle and lower quantiles (<50th) (Figure 1a and 1b). As shown in Figure 1c and
 173 1d, though the magnitude and uncertainty of global CHL trends differ by quantile level,
 174 most of the quantile levels show an increase in CHL. All trends are shown after remov-
 175 ing serial correlation.

176 For the OC-CCI data product, all quantiles present a positive and significant trend
 177 (Figure 1a and 1c). The CHL trends in upper quantile (95th) is the steepest with a mag-
 178 nitude of $2.5 \times 10^{-4} \text{ mg m}^{-3} \text{ yr}^{-1}$, whereas the lower and middle quantiles show trends
 179 with smaller magnitudes. These features suggest a slight increase in the variance of global
 180 CHL given a more pronounced increase in the upper quantile than in lower quantiles,
 181 although trend uncertainty is also larger for the 95th quantile. A positive trend of 1.2
 182 $\times 10^{-4} \text{ mg m}^{-3} \text{ yr}^{-1}$ is detected by applying an OLS regression model that is almost
 183 identical to trends in median CHL (50th quantile). It indicates that the average and me-
 184 dian global CHL are changing closely, and at a slightly lower pace than lower and up-
 185 per extreme concentrations. The 95 % confidence intervals in all quantile levels suggest
 186 the larger uncertainty (± 0.5 and $\pm 1.2 \times 10^{-4} \text{ mg m}^{-3} \text{ yr}^{-1}$) in the lower and upper quan-
 187 tiles, compared to middle quantiles with $\pm 0.2 \times 10^{-4} \text{ mg m}^{-3} \text{ yr}^{-1}$.

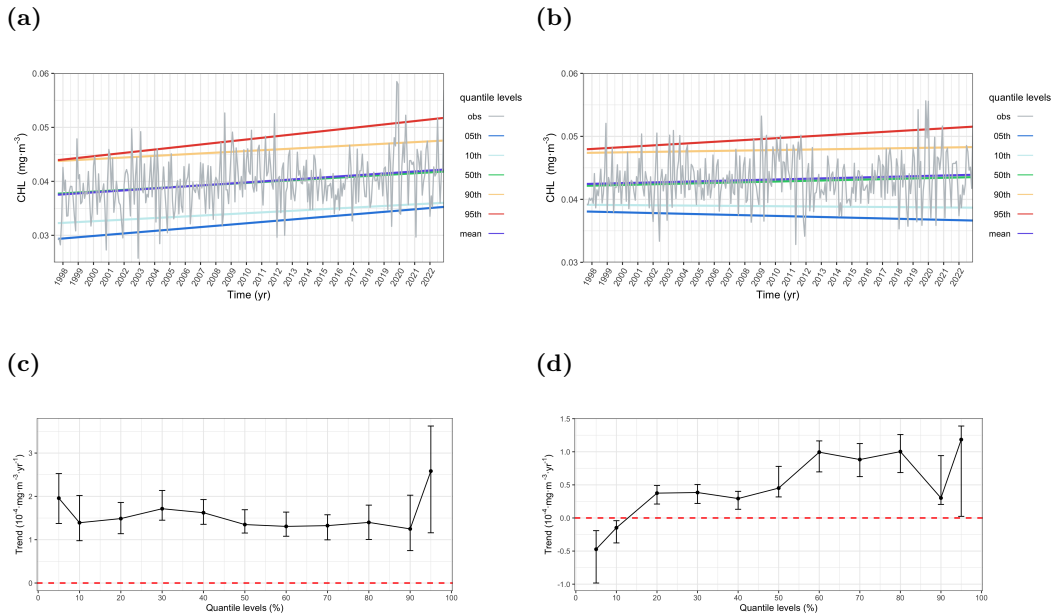


Figure 1 Time series of monthly global mean CHL from 1997-2022 with trends fitted in different quantile levels from (a) OC-CCI product and (b) GlobColour product. Trends in different quantile levels (5th to 95th levels) with 95% confidence intervals from (c) OC-CCI product and (d) GlobColour product. Trends were fitted to transformed data to remove autocorrelation.

188 The trends and their variability in global CHL are similar for most quantiles in the
 189 GlobColour data product (Figure 1b and 1d). Although negative trends are detected in
 190 the 5th and 10th quantile levels, trends in upper and middle quantile levels are positive.
 191 Again, upper quantile levels have a larger uncertainty (Figure 1d). A trend in CHL mean
 192 is $1 \times 10^{-4} \text{ mg m}^{-3} \text{ yr}^{-1}$ that is very similar to trends in median CHL ($0.5 \times 10^{-4} \text{ mg}$
 193 $\text{m}^{-3} \text{ yr}^{-1}$). The difference in trend sign between global CHL high and low imply an in-
 194 creasing variability over this period. This increase in variability is less pronounced in the
 195 OC-CCI dataset, with the lower and upper quantiles having the same trend sign but dif-
 196 ferent magnitudes (Figure 1a). The results are not sensitive to a log-transformation of
 197 CHL (Text S1; Figure S2 in supporting information).

198 3.2 Regional Trends

199 Trends estimated in each grid cell are presented in Figure 2. After a preliminary
 200 analysis, the presence of autocorrelation was detected in most areas of the ocean (Fig-
 201 ure S3 in the supporting information). As such, a Cochrane-Orcutt transformation was
 202 applied to remove autocorrelation from the data. It must be noted that this transfor-
 203 mation does not remove the trend signal, but only sieve the autocorrelation. As a com-
 204 parison, a different transformation procedure was used to remove autocorrelation from
 205 the data, the Hildreth-Lu method (Figure S1 in the supporting information). Results
 206 are consistent with the Cochrane-Orcutt transformation (Text S1; Figure S1 in the sup-
 207 porting information), suggesting that the results are robust to the choice of transforma-
 208 tion approach.

209 At the regional scale, trends in lower quantiles are more scattered (Figure 2a and
 210 2b), and patterns become more apparent in the median and larger quantiles (Figure 2c,

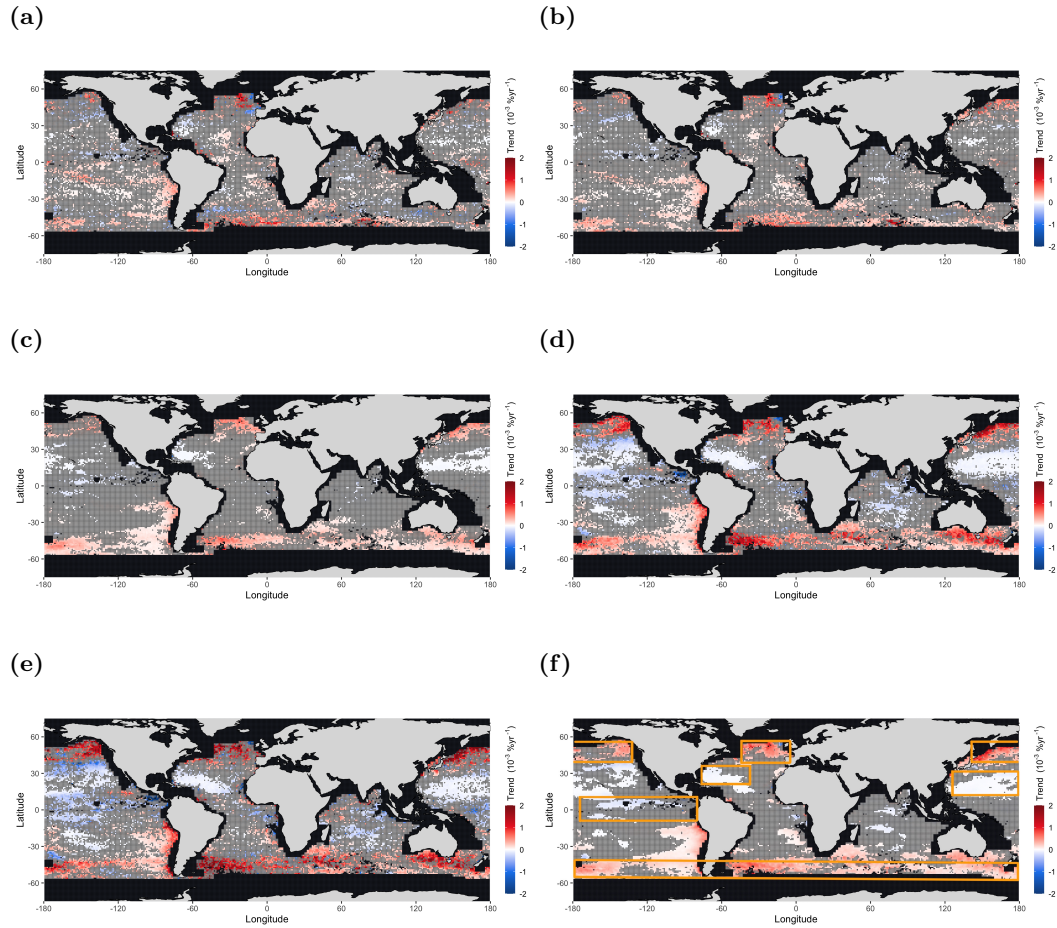


Figure 2 Maps of CHL trends from the OC-CCI data product during 1997-2022 in (a) 5th, (b) 10th, (c) 50th, (d) 90th, (e) 95th quantile levels, and (f) in CHL mean, respectively. Trends were fitted to transformed data to remove autocorrelation via the Cochrane-Orcutt procedure. The grey shadows are regions where trends are not significant at a 5% level.

211 2d, and 2e). Overall, regions with significant trends in the upper quantiles are mainly
 212 located at high latitudes (+), in equatorial (-), and oligotrophic regions (-) (Figure 2d
 213 and 2e). A few regions emerge with consistent patterns of change in North Pacific Sub-
 214 arctic Province, North Atlantic Drift Province, Subantarctic Province, Pacific Equato-
 215 rial Province, North Pacific Subtropical Gyre, and North Atlantic Subtropical Gyre, and
 216 are highlighted in Figure 2f. The regions are divided as defined by Longhurst (1995) (see
 217 supporting information, Text S3).

218 In Figure 3, we further look into the regions with significant trends identified above.
 219 We averaged grid cells in these regions and estimated trends with their respective con-
 220 fidence intervals. Trends in different quantiles may vary in magnitude and sign, suggest-
 221 ing that the shape of the CHL distribution is varying on a regional scale. Positive trends
 222 dominate in the North Pacific Subarctic Province, North Atlantic Drift Province, and
 223 Subantarctic Province (Figure 3a, 3b, and 3c). Trends in Subantarctic Province are pos-
 224 itive in all quantile levels, while the North Pacific Subarctic Province and North Atlantic
 225 Drift Province exhibit similar patterns whereby trends in lower quantiles are not signif-
 226 icant and median and upper quantiles are significant and positive. In these three regions,
 227 trends detected in different quantiles are consistent with an increasing variability over
 228 the observational record. In low nutrient regions, namely the Pacific Equatorial Province
 229 and North Pacific Subtropical Gyre, trends in the lower quantiles are significantly in-
 230 creasing even if negative trends are observed in the mean/median (Figure 3d and 3e).
 231 It might indicate that CHL low extremes become less frequent during the recording pe-
 232 riod. Among these regions, Pacific Equatorial Province and North Pacific Subtropical
 233 Gyre present consistent trends with an overall decrease in variability. The North Atlantic
 234 Subtropical Gyre exhibits decreasing trends in middle quantile levels and increasing trends
 235 at upper quantiles, suggesting a slightly increasing variance over time. Trend estimates
 236 obtained by the OLS model closely follow those for the median in all of the regions (see
 237 supporting information, Figure S4).

238 Most regions show increasing variability in CHL except Pacific Equatorial and North
 239 Pacific Subtropical Gyre Province. The large variance of CHL relates to climate season-
 240 ality and dominates at high latitudes, sub-polar, and coastal waters. December, January,
 241 and February (DJF) and June, July, and August (JJA) are two seasons that are com-
 242 monly used to analyze ocean phytoplankton blooms because they represent contrasting
 243 environmental conditions that affect the growth and distribution of phytoplankton in the
 244 ocean. The impact of regional seasonality is shown in the supporting information (Text
 245 S1; Figure S5).

246 We also include results obtained on the GlobColour dataset in these regions to as-
 247 sess the sensitivity of our findings to the choice of the dataset in Text S2 (supporting
 248 information). In most regions, trends detected in different quantiles are consistent ex-
 249 cept for the North Atlantic Drift province and the North Pacific Subtropical Gyre Province
 250 (Figure S6, S7, and S8 in the supporting information).

251 4 Discussion and Conclusion

252 In this study, we provide a first assessment of changes in CHL distribution in the
 253 global ocean over the 1997–2022 period. At the global scale, our results suggest that dif-
 254 ferent quantiles are changing at different paces, with CHL high extremes changing faster
 255 than the rest of the distribution. This difference in pace results in an overall slight in-
 256 crease in CHL variability. At the regional scale, CHL high extremes are increasing at high
 257 latitudes and decreasing in equatorial and oligotrophic regions. These changes are con-
 258 sistent with Earth System Models projections whereby high latitude oceans are light-
 259 limited while equatorial and oligotrophic regions are limited by nutrients (Doney, 2006;
 260 Doney et al., 2012; Kwiatkowski et al., 2020). Furthermore, we show that changes at high
 261 latitudes are more pronounced during DJF season, while changes in equatorial regions

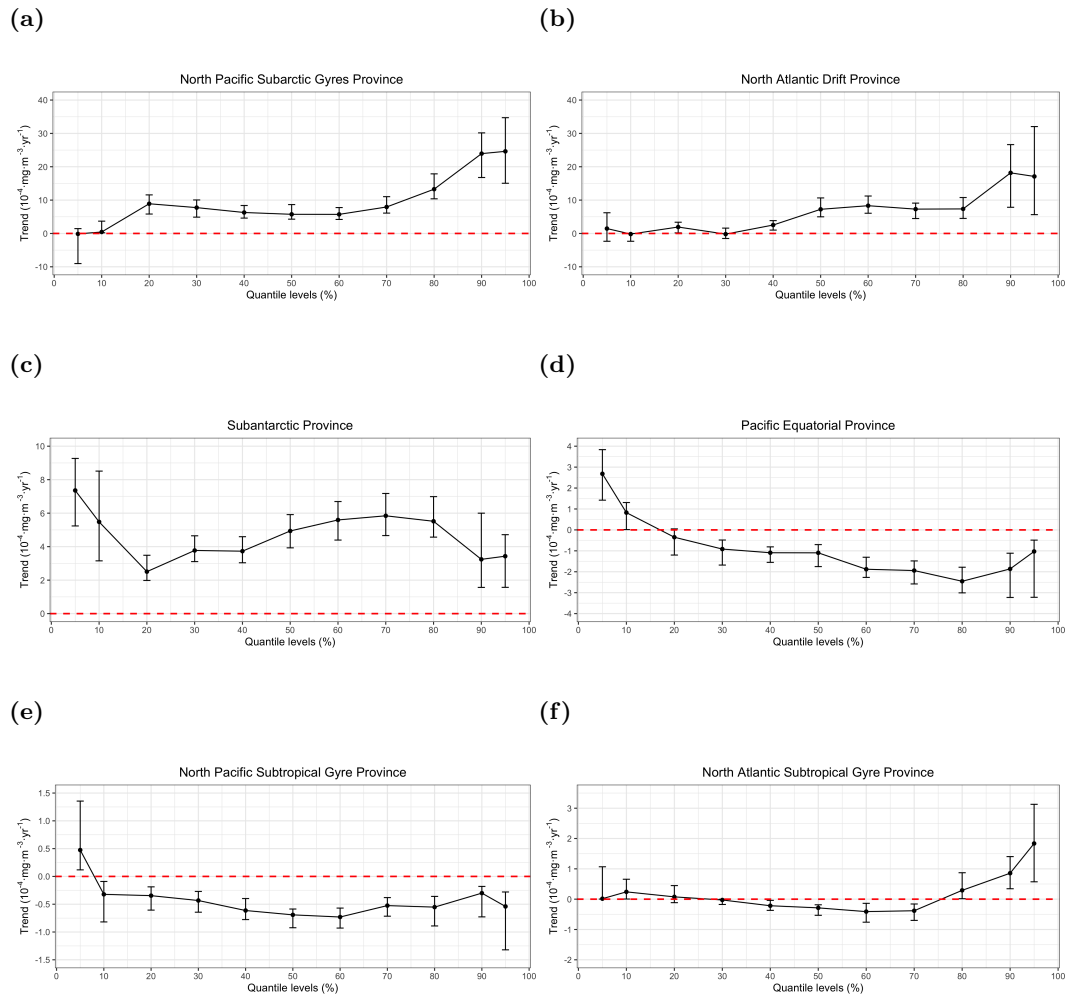


Figure 3 Regional CHL trends in OC-CCI data product in different quantile levels in regions, (a) North Pacific Subarctic Gyre Province, (b) North Atlantic Drift Province, (c) Subantarctic Province, (d) Pacific Equatorial Province, (e) North Pacific Subtropical Gyre Province, and (f) North Atlantic Subtropical Gyre Province. The 95% confidence intervals for each regression are represented by the vertical lines. The red horizontal dashed line is zero.

262 dominate during JJA. This may be due to climate processes like El Niño-Southern Os-
263 cillation (ENSO) that tend to start during JJA in equatorial regions.

264 In a study focusing on analyzing phytoplankton carbon biomass in an Earth Sys-
265 tem Model large ensemble, Elsworth et al. (2022) identified decreasing variability of global
266 phytoplankton variance from 1920-2100. Our results do not show an overall decreased
267 variability in CHL. This difference may be due to the differing periods of analysis. In-
268 deed, our analysis focuses on the period 1997-2022, and changes detected over that pe-
269 riod may be more indicative of decadal variability rather than long-term impact of cli-
270 mate change over 1920-2100. Another explanation could be that the two studies are an-
271 alyzing different variables. While previous studies have discussed the correlation between
272 the spatial distribution of CHL (used in this study) and phytoplankton carbon biomass
273 (Kostadinov et al., 2016; Martínez-Vicente et al., 2017), those variables tend to decou-
274 ple especially in subtropical regions (Barbieux et al., 2018). Future work should focus
275 on analyzing CHL extremes and variability in models to assess whether long-term changes
276 in CHL variability and extremes are consistent with observations, in order to better un-
277 derstand their drivers and anticipate future changes.

278 Regional trends differ from those at the global scale with mixed signs and larger
279 magnitudes. Regions with significant trends in upper quantiles include the North Pa-
280 cific Subarctic Province (+), North Atlantic Drift Province (+), Subantarctic Province
281 (+), Pacific Equatorial Province (-), North Pacific Subtropical Gyre (-), and North At-
282 lantic Subtropical Gyre (-), as shown in Figure 2f. Regional changes in upper quantiles
283 described above also correspond to changes in CHL variability with increase in the North
284 Pacific Subarctic Province, North Atlantic Drift Province, and Subantarctic Provinces,
285 and declining variability in Pacific Equatorial and North Pacific Subtropical Gyre Province.
286 Those regions are characterized by noticeable ecological and biogeochemical seasonal vari-
287 ability that is closely related to strong annual cycles in light, nutrients, temperature, wind
288 force, and zooplankton grazing at surface (Henson et al., 2010; Elsworth et al., 2022).
289 At the regional scale, large-scale climate patterns such as El Niño Southern Oscillation
290 (ENSO), Pacific Decadal Oscillation (PDO), and North Atlantic Oscillation (NAO) are
291 known drivers of CHL trends and variability (Corno et al., 2007; Zhai et al., 2013; Kang
292 et al., 2017; Gao et al., 2020; Le Grix et al., 2021). In the North Pacific Subarctic Gyres
293 and North Atlantic Drift Provinces, warming over the last two decades has resulted in
294 more phytoplankton blooming (Dunstan et al., 2018). Our results showing that CHL high
295 extremes are becoming more frequent are consistent with Dunstan et al. (2018) and Kahru
296 & Mitchell (2008) findings. Changes in the North Atlantic Drift region are more pronounced
297 than the North Pacific Subarctic Gyre, also consistent with previous analysis on phy-
298 toplankton blooms (Westberry et al., 2016). As for the Southern hemisphere, seasonal
299 variation in the location of transition zones between subpolar and subtropical gyres co-
300 incide with increasing CHL variance (Dunstan et al., 2018). This phenomenon may in-
301 dicate that the increasing seasonal variance plays a role in the CHL distribution changes
302 detected here (Thomalla et al., 2023). Trends in Subantarctic Province are significantly
303 positive in all quantile levels. A possible explanation is that though iron limitation con-
304 trols the Southern Ocean, sea surface warming could still be an important driver on sea-
305 sonal phytoplankton blooms in this region instead of light or nutrients (Moore et al., 2013;
306 Laufkötter et al., 2015), resulting in positive and similar magnitude changes in CHL dis-
307 tribution and their variability over the observational period.

308 Some limitations in this study may impact the validity of our results. First, the short-
309 ness of the record may impact our results, as we use observations over a period that is
310 slightly shorter (26 years) than the recommended 30 years for assessing climate change
311 impacts (WMO, 2018). More specifically, satellite ocean color datasets require multiple
312 decades to distinguish long-term climate-related trends from natural variability (Henson
313 et al., 2010; Beaulieu et al., 2013; Bindoff et al., 2022), although exact detection timescales
314 vary depending on regional interannual and decadal variability and magnitude of trends

315 (Henson et al., 2010). That said, previous studies aimed at estimating timescales of trend
316 detection in ocean CHL (Henson et al., 2010; Beaulieu et al., 2013) focused on mean changes
317 in CHL, not variability and extremes, and these detection times may be different here.
318 Recent studies also suggested that long-term trends in satellite ocean color may be de-
319 tectable faster in reflectance rather than CHL (Cael et al., 2023; Dutkiewicz et al., 2019).
320 Assessing whether similar patterns can be detected in reflectance observations should
321 be the focus of a future study.

322 Second, merged time series of multimission products used here are susceptible to
323 biases, which may impact the CHL trends detected (Saulquin et al., 2013; Mélin, 2016;
324 Mélin et al., 2017; Hammond et al., 2018). GlobColour merges multi-sensor CHL with
325 a specific flagging, but is not explicitly bias-corrected (Maritorena et al., 2010; Garnes-
326 son et al., 2019; Yu et al., 2023). For the OC-CCI product, multi-sensors reflectance is
327 merged before CHL derivation, which results in a more constrained approach (Sathyendranath
328 et al., 2017). As a result, long-term CHL trends detected in OC-CCI and Glob-
329 Colour products differ in some regions (e.g., North Pacific Subarctic Gyre and North At-
330 lantic Drift Provinces). By utilizing the two datasets, we reduce the sensitivity of our
331 results to the choice of datasets and bias correction algorithms, but we cannot entirely
332 eliminate the possibility of bias in trends detected introduced from using multiple mis-
333 sion data products.

334 Third, few studies have used satellite-derived CHL datasets to analyze extremes
335 (Le Grix et al., 2021; Woolway et al., 2021). Bias due to high solar zenith angles, clouds,
336 and aerosols may affect the data (Le Grix et al., 2021; Gregg et al., 2009). Low sampling
337 rates of CHL extremes may also affect our results. The majority of the surface ocean is
338 characterized by low CHL levels in the Oligotrophic area, whereas high CHL levels are
339 only present in a small portion ($\sim 1\%$) primarily located in coastal zones (Sathyendranath
340 et al., 2019; Van Oostende et al., 2018). Insufficient data in CHL extremes correspond-
341 ing to lower and upper quantile levels result in higher uncertainties (larger confidence
342 intervals) for CHL trends.

343 Finally, we made assumptions when fitting the statistical model that may influence
344 the results. We assume that trends in different quantiles are linear, following previous
345 studies (Gregg et al., 2005; Boyce et al., 2010; Henson et al., 2010; Boyce et al., 2010;
346 Saulquin et al., 2013; Mélin, 2016; Henson et al., 2016; Hammond et al., 2020). More com-
347 plex time dependence such as nonlinear trends or abrupt changes were not assessed as
348 linear trends can provide a first-order approximation to long-term changes and avoid over-
349 fitting the data. Furthermore, the period of observations is quite short, so there is a risk
350 of overfitting with more complex time dependence. A constant seasonal pattern is as-
351 sumed in our study, though some studies have shown that the CHL seasonal cycle might
352 vary over time (Vantrepotte & Mélin, 2009; Henson et al., 2013). A changing seasonal
353 cycle over the period of observation may bias trends detected here. However, changes
354 in seasonal cycle require longer time series to be detected than trends in the mean (Hen-
355 son et al., 2013), and potential biases introduced here should be minimal. Quantile re-
356 gression models used here assume independent errors. To deal with the presence of au-
357 tocorrelation, we used pre-whitening methods. These approaches help reduce the risk
358 of a false detection (i.e., detecting a trend when there is none), but are also associated
359 with a reduced power of detection (Bayazit & Önöz, 2007). As such, significant trends
360 may not be detected. Results may also differ based on the pre-whitening approach used.
361 Here, we reduced this problem by using two different pre-whitening approaches, Cochran-
362 Orcutt and Hildreth-Lu procedures, and showed our results were not sensitive to the choice
363 of pre-whitening method (see supporting information).

364 To our knowledge, this is the first study assessing long-term changes in CHL dis-
365 tribution on a global scale, as opposed to focusing entirely on mean CHL. More infor-
366 mation related to climate variables such as seasonal changes and their variability, as well
367 as extreme conditions, are revealed by assessing trends in all quantile levels of the CHL

368 distribution. We conclude that over the satellite record, trends in CHL extremes are more
 369 pronounced than that in the mean CHL. Henson et al. (2010) concluded that the cur-
 370 rent length of observation recording is insufficient to identify a climate change trend in
 371 mean CHL and suggested that a time series of approximately 40 years is needed to sep-
 372 arate a global warming trend from natural variability. Our results show that trends in
 373 CHL high extremes tend to have larger magnitudes and uncertainties than trends in the
 374 mean, both of which may impact detection times. By considering the whole distribution
 375 (not just the mean), we may be able to detect climate change-related trends faster and
 376 more holistically, and better understand the effects of anthropogenic forcing on marine
 377 ecosystems, which will enable us to make more effective decisions concerning socioeco-
 378 nomic systems that are affected by climate change (Henson et al., 2016). Future work
 379 should focus on quantifying detection times in different aspects of CHL distribution to
 380 develop the ability to formally detect the impact of climate change in marine ecosystems
 381 as soon as possible.

382 5 Open Research

383 Data Availability Statement

384 The OC-CCI data can be found on the open portal of ESA’s climate office at this
 385 site: <http://dx.doi.org/10.5285/1dbe7a109c0244aaad713e078fd3059a>. The Glob-
 386 Colour data can be found on the GlobColour Project of Copernicus program at this site:
 387 <https://doi.org/10.48670/moi-00281>. The R code used to produce the initial dataset,
 388 statistically analyze the quantile regression model, and reproduce the figures of the manuscript,
 389 is publicly available at <https://doi.org/10.5281/zenodo.8343435>.

390 Acknowledgments

391 We would like to thank the Ocean-Colour Climate Change Initiative and the Glob-
 392 Colour Project for making their data publicly available. DZ acknowledges financial sup-
 393 port from the program of the China Scholarship Council No. 20200801001. CB thanks
 394 National Science Foundation Grant AGS-2143550 for partial support. RK thanks NASA
 395 Grant 80NSSC21K165 for partial support.

396 References

- 397 Abbas, S. A., Xuan, Y., & Song, X. (2019). Quantile regression based methods for
 398 investigating rainfall trends associated with flooding and drought conditions. *Wa-*
 399 *ter Resources Management*, *33*, 4249–4264.
- 400 Alexander, M. A., Scott, J. D., Friedland, K. D., Mills, K. E., Nye, J. A., Persh-
 401 ing, A. J., & Thomas, A. C. (2018). Projected sea surface temperatures over
 402 the 21st century: Changes in the mean, variability and extremes for large marine
 403 ecosystem regions of northern oceans. *Elementa: Science of the Anthropocene*, *6*.
- 404 Barbieux, M., Uitz, J., Bricaud, A., Organelli, E., Poteau, A., Schmechtig, C., . . .
 405 others (2018). Assessing the variability in the relationship between the particu-
 406 late backscattering coefficient and the chlorophyll a concentration from a global
 407 biogeochemical-argo database. *Journal of Geophysical Research: Oceans*, *123*(2),
 408 1229–1250.
- 409 Barbosa, S. M. (2008). Quantile trends in baltic sea level. *Geophysical Research Let-*
 410 *ters*, *35*(22).
- 411 Bayazit, M., & Önöz, B. (2007). To prewhiten or not to prewhiten in trend analysis?
 412 *Hydrological Sciences Journal*, *52*(4), 611–624.
- 413 Beaulieu, C., Henson, S. A., Sarmiento, J. L., Dunne, J. P., Doney, S. C.,
 414 Rykaczewski, R. R., & Bopp, L. (2013). Factors challenging our ability to de-
 415 tect long-term trends in ocean chlorophyll. *Biogeosciences*, *10*(4), 2711–2724.
- 416 Bindoff, N., Cheung, W., Kairo, J., Aristegui, J., Guinder, V., Hallberg, R., . . .

- 417 Williamson, P. (2022). Changing ocean, marine ecosystems, and dependent com-
 418 munities. In *The ocean and cryosphere in a changing climate: Special report of the*
 419 *intergovernmental panel on climate change* (p. 447–587). Cambridge, UK and New
 420 York, NY: Cambridge University Press. doi: 10.1017/9781009157964.007
- 421 Blondeau-Patissier, D., Gower, J. F., Dekker, A. G., Phinn, S. R., & Brando, V. E.
 422 (2014). A review of ocean color remote sensing methods and statistical techniques
 423 for the detection, mapping and analysis of phytoplankton blooms in coastal and
 424 open oceans. *Progress in oceanography*, *123*, 123–144.
- 425 Bojinski, S., Verstraete, M., Peterson, T. C., Richter, C., Simmons, A., & Zemp, M.
 426 (2014). The concept of essential climate variables in support of climate research,
 427 applications, and policy. *Bulletin of the American Meteorological Society*, *95*(9),
 428 1431–1443.
- 429 Bopp, L., Resplandy, L., Orr, J. C., Doney, S. C., Dunne, J. P., Gehlen, M., . . . oth-
 430 ers (2013). Multiple stressors of ocean ecosystems in the 21st century: projections
 431 with cmip5 models. *Biogeosciences*, *10*(10), 6225–6245.
- 432 Boyce, D. G., Lewis, M. R., & Worm, B. (2010). Global phytoplankton decline over
 433 the past century. *Nature*, *466*(7306), 591–596.
- 434 Burger, F. A., Terhaar, J., & Frölicher, T. L. (2022). Compound marine heatwaves
 435 and ocean acidity extremes. *Nature Communications*, *13*(1), 4722.
- 436 Cael, B., Bisson, K., Boss, E., Dutkiewicz, S., & Henson, S. (2023). Global climate-
 437 change trends detected in indicators of ocean ecology. *Nature*, 1–4.
- 438 Cai, Y., & Reeve, D. E. (2013). Extreme value prediction via a quantile function
 439 model. *Coastal Engineering*, *77*, 91–98.
- 440 Cochran, D., & Orcutt, G. H. (1949). Application of least squares regression to re-
 441 lationships containing auto-correlated error terms. *Journal of the American statisti-*
 442 *cal association*, *44*(245), 32–61.
- 443 Corno, G., Karl, D. M., Church, M. J., Letelier, R. M., Lukas, R., Bidigare, R. R.,
 444 & Abbott, M. R. (2007). Impact of climate forcing on ecosystem processes in
 445 the north pacific subtropical gyre. *Journal of Geophysical Research: Oceans*,
 446 *112*(C4).
- 447 Doney, S. C. (2006). Plankton in a warmer world. *Nature*, *444*(7120), 695–696.
- 448 Doney, S. C., Ruckelshaus, M., Emmett Duffy, J., Barry, J. P., Chan, F., English,
 449 C. A., . . . others (2012). Climate change impacts on marine ecosystems. *Annual*
 450 *review of marine science*, *4*, 11–37.
- 451 Dufour, J.-M., Gaudry, M. J., & Liem, T. C. (1980). The cochrane-orcutt procedure
 452 numerical examples of multiple admissible minima. *Economics Letters*, *6*(1), 43–
 453 48.
- 454 Dunstan, P. K., Foster, S. D., King, E., Risbey, J., O’Kane, T. J., Monselesan, D.,
 455 . . . Thompson, P. A. (2018). Global patterns of change and variation in sea
 456 surface temperature and chlorophyll a. *Scientific reports*, *8*(1), 14624.
- 457 Dutkiewicz, S., Hickman, A. E., Jahn, O., Henson, S. A., Beaulieu, C., & Monier, E.
 458 (2019). Ocean colour signature of climate change. *Nature communications*, *10*(1),
 459 578.
- 460 Elsworth, G. W., Lovenduski, N. S., Krumhardt, K. M., Marchitto, T. M., &
 461 Schlunegger, S. (2022). Anthropogenic climate change drives non-stationary
 462 phytoplankton variance. *EGU sphere*, 1–21.
- 463 Field, C. B., Behrenfeld, M. J., Randerson, J. T., & Falkowski, P. (1998). Primary
 464 production of the biosphere: integrating terrestrial and oceanic components. *sci-*
 465 *ence*, *281*(5374), 237–240.
- 466 Free, C. M., Thorson, J. T., Pinsky, M. L., Oken, K. L., Wiedenmann, J., & Jensen,
 467 O. P. (2019). Impacts of historical warming on marine fisheries production.
 468 *Science*, *363*(6430), 979–983.
- 469 Gao, N., Ma, Y., Zhao, M., Zhang, L., Zhan, H., Cai, S., & He, Q. (2020). Quantile
 470 analysis of long-term trends of near-surface chlorophyll-a in the pearl river plume.

- 471 *Water*, 12(6), 1662.
- 472 Garnesson, P., Mangin, A., Fanton d’Andon, O., Demaria, J., & Bretagnon, M.
473 (2019). The cmems globcolour chlorophyll a product based on satellite obser-
474 vation: Multi-sensor merging and flagging strategies. *Ocean Science*, 15(3),
475 819–830.
- 476 Gregg, W. W., Casey, N. W., & McClain, C. R. (2005). Recent trends in global
477 ocean chlorophyll. *Geophysical research letters*, 32(3).
- 478 Gregg, W. W., Casey, N. W., O’Reilly, J. E., & Esaias, W. E. (2009). An empir-
479 ical approach to ocean color data: Reducing bias and the need for post-launch
480 radiometric re-calibration. *Remote Sensing of Environment*, 113(8), 1598–1612.
- 481 Gruber, N., Boyd, P. W., Frölicher, T. L., & Vogt, M. (2021). Biogeochemical ex-
482 tremes and compound events in the ocean. *Nature*, 600(7889), 395–407.
- 483 Hammond, M. L., Beaulieu, C., Henson, S. A., & Sahu, S. K. (2018). Assessing the
484 presence of discontinuities in the ocean color satellite record and their effects on
485 chlorophyll trends and their uncertainties. *Geophysical Research Letters*, 45(15),
486 7654–7662.
- 487 Hammond, M. L., Beaulieu, C., Henson, S. A., & Sahu, S. K. (2020). Regional
488 surface chlorophyll trends and uncertainties in the global ocean. *Scientific reports*,
489 10(1), 15273.
- 490 Henson, S. A., Beaulieu, C., & Lampitt, R. (2016). Observing climate change trends
491 in ocean biogeochemistry: when and where. *Global change biology*, 22(4), 1561–
492 1571.
- 493 Henson, S. A., Cole, H., Beaulieu, C., & Yool, A. (2013). The impact of global
494 warming on seasonality of ocean primary production. *Biogeosciences*, 10(6), 4357–
495 4369.
- 496 Henson, S. A., Sarmiento, J. L., Dunne, J. P., Bopp, L., Lima, I., Doney, S. C., ...
497 Beaulieu, C. (2010). Detection of anthropogenic climate change in satellite records
498 of ocean chlorophyll and productivity. *Biogeosciences*, 7(2), 621–640.
- 499 Hildreth, C., & Lu, J. (1960). Demand relations with autocorrelated distur-
500 bances. *Technical Bulletin. Michigan State University Agricultural Experiment*
501 *Station*(276).
- 502 Hollmann, R., Merchant, C. J., Saunders, R., Downy, C., Buchwitz, M., Cazenave,
503 A., ... others (2013). The esa climate change initiative: Satellite data records
504 for essential climate variables. *Bulletin of the American Meteorological Society*,
505 94(10), 1541–1552.
- 506 Huo, L., Kim, T.-H., Kim, Y., & Lee, D. J. (2017). A residual-based test for auto-
507 correlation in quantile regression models. *Journal of Statistical Computation and*
508 *Simulation*, 87(7), 1305–1322.
- 509 Kahru, M., & Mitchell, B. G. (2008). Ocean color reveals increased blooms in var-
510 ious parts of the world. *Eos, Transactions American Geophysical Union*, 89(18),
511 170–170.
- 512 Kang, X., Zhang, R.-H., Gao, C., & Zhu, J. (2017). An improved enso simulation
513 by representing chlorophyll-induced climate feedback in the ncar community earth
514 system model. *Scientific Reports*, 7(1), 17123.
- 515 Koenker, R., & Bassett Jr, G. (1978). Regression quantiles. *Econometrica: journal*
516 *of the Econometric Society*, 33–50.
- 517 Koenker, R., Chernozhukov, V., He, X., & Peng, L. (2017). *Handbook of quantile re-*
518 *gression*. CRC press.
- 519 Koenker, R., & D’Orey, V. (1987). *Computing regression quantiles, applied statis-*
520 *tics*.
- 521 Koenker, R., & Hallock, K. F. (2001). Quantile regression. *Journal of economic per-*
522 *spectives*, 15(4), 143–156.
- 523 Koenker, R., Portnoy, S., Ng, P. T., Zeileis, A., Grosjean, P., & Ripley, B. D. (2018).
524 Package ‘quantreg’. *Cran R-project. org*.

- 525 Kostadinov, T. S., Milutinović, S., Marinov, I., & Cabré, A. (2016). Carbon-based
 526 phytoplankton size classes retrieved via ocean color estimates of the particle size
 527 distribution. *Ocean Science*, *12*(2), 561–575.
- 528 Kwiatkowski, L., Torres, O., Bopp, L., Aumont, O., Chamberlain, M., Christian,
 529 J. R., ... others (2020). Twenty-first century ocean warming, acidification, deoxy-
 530 genation, and upper-ocean nutrient and primary production decline from cmip6
 531 model projections. *Biogeosciences*, *17*(13), 3439–3470.
- 532 Landschützer, P., Gruber, N., Bakker, D. C., Stemmler, I., & Six, K. D. (2018).
 533 Strengthening seasonal marine co2 variations due to increasing atmospheric co2.
 534 *Nature Climate Change*, *8*(2), 146–150.
- 535 Laufkötter, C., Vogt, M., Gruber, N., Aita-Noguchi, M., Aumont, O., Bopp, L.,
 536 ... others (2015). Drivers and uncertainties of future global marine primary
 537 production in marine ecosystem models. *Biogeosciences*, *12*(23), 6955–6984.
- 538 Le Grix, N., Zscheischler, J., Laufkötter, C., Rousseaux, C. S., & Frölicher, T. L.
 539 (2021). Compound high-temperature and low-chlorophyll extremes in the ocean
 540 over the satellite period. *Biogeosciences*, *18*(6), 2119–2137.
- 541 Longhurst, A. (1995). Seasonal cycles of pelagic production and consumption.
 542 *Progress in oceanography*, *36*(2), 77–167.
- 543 Maritorena, S., d’Andon, O. H. F., Mangin, A., & Siegel, D. A. (2010). Merged
 544 satellite ocean color data products using a bio-optical model: Characteristics,
 545 benefits and issues. *Remote Sensing of Environment*, *114*(8), 1791–1804.
- 546 Martínez-Vicente, V., Evers-King, H., Roy, S., Kostadinov, T. S., Tarran, G. A.,
 547 Graff, J. R., ... others (2017). Intercomparison of ocean color algorithms for
 548 picophytoplankton carbon in the ocean. *Frontiers in Marine Science*, *4*, 378.
- 549 McClain, C. R. (2009). A decade of satellite ocean color observations. *Annual Re-
 550 view of Marine Science*, *1*, 19–42.
- 551 Mélin, F. (2016). Impact of inter-mission differences and drifts on chlorophyll-a
 552 trend estimates. *International Journal of Remote Sensing*, *37*(10), 2233–2251.
- 553 Mélin, F., Vantrepotte, V., Chuprin, A., Grant, M., Jackson, T., & Sathyendranath,
 554 S. (2017). Assessing the fitness-for-purpose of satellite multi-mission ocean color
 555 climate data records: A protocol applied to oc-cci chlorophyll-a data. *Remote
 556 Sensing of Environment*, *203*, 139–151.
- 557 Moore, C., Mills, M., Arrigo, K., Berman-Frank, I., Bopp, L., Boyd, P., ... others
 558 (2013). Processes and patterns of oceanic nutrient limitation. *Nature geoscience*,
 559 *6*(9), 701–710.
- 560 Rodgers, K. B., Lee, S.-S., Rosenbloom, N., Timmermann, A., Danabasoglu, G.,
 561 Deser, C., ... others (2021). Ubiquity of human-induced changes in climate
 562 variability. *Earth System Dynamics*, *12*(4), 1393–1411.
- 563 Sankarasubramanian, A., & Lall, U. (2003). Flood quantiles in a changing climate:
 564 Seasonal forecasts and causal relations. *Water Resources Research*, *39*(5).
- 565 Sarmiento, J. L., Slater, R., Barber, R., Bopp, L., Doney, S., Hirst, A., ... others
 566 (2004). Response of ocean ecosystems to climate warming. *Global Biogeochemical
 567 Cycles*, *18*(3).
- 568 Sathyendranath, S., Brewin, R. J., Brockmann, C., Brotas, V., Calton, B., Chuprin,
 569 A., ... others (2019). An ocean-colour time series for use in climate studies: the
 570 experience of the ocean-colour climate change initiative (oc-cci). *Sensors*, *19*(19),
 571 4285.
- 572 Sathyendranath, S., Brewin, R. J., Jackson, T., Mélin, F., & Platt, T. (2017).
 573 Ocean-colour products for climate-change studies: What are their ideal character-
 574 istics? *Remote Sensing of Environment*, *203*, 125–138.
- 575 Saulquin, B., Fablet, R., Mangin, A., Mercier, G., Antoine, D., & Fanton d’Andon,
 576 O. (2013). Detection of linear trends in multisensor time series in the presence of
 577 autocorrelated noise: Application to the chlorophyll-a seawifs and meris data sets
 578 and extrapolation to the incoming sentinel 3-olci mission. *Journal of Geophysical*

- 579 *Research: Oceans*, 118(8), 3752–3763.
- 580 Tareghian, R., & Rasmussen, P. (2013). Analysis of arctic and antarctic sea ice ex-
581 tent using quantile regression. *International Journal of Climatology*, 33(5), 1079–
582 1086.
- 583 Thomalla, S. J., Nicholson, S.-A., Ryan-Keogh, T. J., & Smith, M. E. (2023).
584 Widespread changes in southern ocean phytoplankton blooms linked to climate
585 drivers. *Nature Climate Change*, 1–10.
- 586 Van Oostende, N., Dussin, R., Stock, C., Barton, A., Curchitser, E., Dunne, J. P., &
587 Ward, B. (2018). Simulating the ocean’s chlorophyll dynamic range from coastal
588 upwelling to oligotrophy. *Progress in oceanography*, 168, 232–247.
- 589 Vantrepotte, V., & Mélin, F. (2009). Temporal variability of 10-year global seawifs
590 time-series of phytoplankton chlorophyll a concentration. *ICES Journal of Marine
591 Science*, 66(7), 1547–1556.
- 592 Westberry, T. K., Schultz, P., Behrenfeld, M. J., Dunne, J. P., Hiscock, M. R., Mar-
593 itorena, S., ... Siegel, D. A. (2016). Annual cycles of phytoplankton biomass
594 in the subarctic atlantic and pacific ocean. *Global Biogeochemical Cycles*, 30(2),
595 175–190.
- 596 WMO. (2018). *Guide to climatological practices*. World Meteorological Organiza-
597 tion.
- 598 Woolway, R. I., Kraemer, B. M., Zscheischler, J., & Albergel, C. (2021). Compound
599 hot temperature and high chlorophyll extreme events in global lakes. *Environmental
600 Research Letters*, 16(12), 124066.
- 601 Yu, S., Bai, Y., He, X., Gong, F., & Li, T. (2023). A new merged dataset of global
602 ocean chlorophyll-a concentration for better trend detection. *Frontiers in Marine
603 Science*, 10, 1051619.
- 604 Zhai, L., Platt, T., Tang, C., Sathyendranath, S., & Walne, A. (2013). The response
605 of phytoplankton to climate variability associated with the north atlantic oscilla-
606 tion. *Deep Sea Research Part II: Topical Studies in Oceanography*, 93, 159–168.